Advances in Science and Technology Research Journal

Advances in Science and Technology Research Journal 2022, 16(6), 23–35
https://doi.org/10.12913/22998624/155168
ISSN 2299-8624, License CC-BY 4.0

Received: 2022.09.15
Accepted: 2022.11.17
Published: 2022.12.01

Analysis of Static Stability and Maneuverability of a New Type of Gyroplane

Tomasz Łusiak[1]

[1] Lublin University of Technology, ul. Nadbystrzycka 38 D, 20-618 Lublin, Poland
* Corresponding author's e-mail: t.lusiak@pollub.pl

ABSTRACT
The paper presents the results of aerodynamic testing and analysis of a new wind-rotor aircraft. The measurements were carried out on a specialized wind tunnel test stand equipped with a dedicated aerodynamic weighing system. Measurements were carried out in an environment corresponding to the real conditions of use of this type of object. A 3D printed model was used for testing.

Keywords: stability, analysis, gyroplane, aerodynamic

INTRODUCTION

The aircraft analysed is a wind-rotorcraft, and to understand the study of the objects it is necessary to familiarise oneself with the characteristics of machines of this type [1]. Wind-gliders belong to the rotorcraft family, their lifting rotor rotates only thanks to autorotation and does not use a motor drive [2]. During take-off, the pilot initiates the rotational movement of the carrier rotor a as a result of the progressive movement resulting from the action of the pushing, or pulling, propeller. The rotor spins to approximately 200 rpm. (prerotation). After a run-up of about 40–50 metres, the lifting force generated on the lifting rotor lifts the aircraft [3].

A prerequisite for the flight of a windscreen aircraft is the continuous blowing of an airstream onto the lifting rotor [4]. Although the wind-glider looks like a helicopter, it is closer to an aircraft. A characteristic of this craft is that it cannot hover, fly sideways or backwards like a helicopter. Instead, take-off and landing are carried out in the manner of an aircraft.

The lifting rotor allows upward and downward flight, and the fuselage tilts to the right and left [15].

Depending on the design, the engine with the propeller can have different locations. Without the engine running, the windmill cannot climb or accelerate. On the other hand, spontaneous autorotation enables full flight control and safe landing [5].

Aircraft of this type are characterised by STOL (short take-off and landing) and unique piloting characteristics. If the limitations of a wind turbine are known and respected, flying it is safe, simple and enjoyable [6].

It contains a description of the methodology for calculating the static (equilibrium) stability of a windmill carrier [7]. Based on the described methodology, a computer software for windmill stability calculations has been developed, which can be used to analyze these issues during the process of designing and preparing for windmill trials. It can also support the interpretation of flight test results and extrapolate test results to other operating conditions. The development of static stability and controllability calculation methodologies has benefited from helicopter experience in this area of issues [8]. The purpose of this paper is to provide a structured knowledge of methods for assessing the stability and maneuverability of a gyrocopter.

STABILITY EQUATIONS

The equations of motion presented below relate to the equilibrium of forces and moments in the coordinate axis system described above [9].

The analysis presented here applies to the windmill with the following components:
a) a single lifting rotor;
b) a trailing or pushing propeller;
c) fuselage;
d) horizontal stabilizer;
e) vertical ballast.

We assume that the control of the rotor is done by tilting and tilting the rotor axis. We denote the angle of tilt of the rotor axis backward from the initial position by A1W (always a positive value), while the angle of tilt of the rotor axis from the plane of symmetry of the windmill is denoted by B1W. The positive value of the B1W angle is taken as the rightward tilt of the rotor axis [10].

The control of the horizontal stabilizer is basically limited to correcting the angle of tilt of the fuselage by changing the attitude angle of the horizontal stabilizer.

The task of static stability is to determine the positions of the windmill control organs in a steady state of flight at which the forces and moments acting on the flying apparatus are zero [11].

$\Sigma X=0$ $\Sigma Y=0$ $\Sigma Z=0$

$\Sigma Mx=0$ $\Sigma My=0$ $\Sigma Mz=0$

Summations take place after all components of the windfarm.

The stability of the windmill can be separated into longitudinal stability and lateral stability [12].

When considering longitudinal stability, we will consider the equations:

$\Sigma X=0$ $\Sigma Y=0$ $\Sigma Mz=0$

and with lateral stability we consider:

$\Sigma Z=0$ $\Sigma Mx=0$ $\Sigma My=0$.

We use the following data for stability analysis [13]:

- geometric, kinematic, and mass parameters of the windframe;
- aerodynamic characteristics of the fuselage, horizontal stabilizer, vertical stabilizer obtained from tunnel tests of the model or from airframe streamlining calculations or from approximate formulas cited in publications on aircraft aerodynamics;
- theoretical or experimental data related to the determination of flux deflection angles on ballasts;
- results of rotor aerodynamic calculations. For stability calculations from rotor calculations, we use the following data:
  - thrust force T;
  - longitudinal force H;
  - lateral force S;
  - rotor angle of attack;
  - inclining moment at the rotor hub Mzp;
  - tilting moment at the rotor hub Mxp.

These values are calculated under rotor autorotation conditions, i.e. Myp = 0.

The process of rotor aerodynamic calculations is performed simultaneously with stability calculations.

LONGITUDINAL STABILITY

For the analysis of longitudinal stability [14], we will use a system of equations that, after decomposition and according to the designations given in Figure 1, takes the form of:

$$\begin{aligned} &-mg\cdot\sin(\upsilon)+T_S\cdot\cos(\varepsilon_s)-\\ &-T\cdot\sin(\alpha-\alpha_k)-H\cdot\cos(\alpha-\alpha_k)+\\ &+Lsp\cdot\sin(\alpha_k-\Delta\varepsilon_{sp})+\\ &-Dsp\cdot\cos(\alpha_k-\Delta\varepsilon_{sp})+\\ &+L_k\cdot\sin(\alpha_k)-D_k\cdot\cos(\alpha_k)=0 \end{aligned} \tag{1}$$

$$\begin{aligned} &-mg\cdot\cos(\upsilon)+T_S\cdot\sin(\varepsilon_s)+\\ &+T\cdot\cos(\alpha-\alpha_k)-H\cdot\sin(\alpha-\alpha_k)+\\ &+Lsp\cdot\cos(\alpha_k-\Delta\varepsilon_{sp})+\\ &+Dsp\cdot\cos(\alpha_k-\Delta\varepsilon_{sp})+\\ &+L_k\cdot\cos(\alpha_k)+D_k\cdot\cos(\alpha_k)=0 \end{aligned} \tag{2}$$

$$Mzs+Mzk+Mzw+Mzsp=0 \tag{3}$$

where: Mzs – means the inclining moment from the propeller,
Mzk – aerodynamic tilting moment of the fuselage without horizontal stabilizer,
Mzw – inclining moment from the lifting rotor,
$Mzsp$ – inclining moment from the horizontal stabilizer.

The following will show the components from the equation of moments (3) according to the accepted designations from Figure 1.

Tilting torque from the propeller

$$Mzs = x_s \cdot Ts \cdot \sin(\varepsilon_s) - y_s \cdot Ts \cdot \cos(\varepsilon_s) \tag{4}$$

Hull leaning moment

$$Mzk = \frac{1}{2}\rho V^2 \cdot F \cdot R \cdot mzk \tag{5}$$

where: F – reference surface when imaging aerodynamic forces and moments of the fuselage – usually it is the surface of the rotor disc,
R – the linear dimension when imaging the aerodynamic forces and moments of the fuselage – usually the rotor radius,
mzk – inclining moment coefficient of the fuselage without horizontal stabilizer

Tilt torque from the rotor

$$\begin{aligned} Mzw = {} & x_w \cdot T \cdot \cos(\alpha - \alpha_k) + \\ & + y_w \cdot T \cdot \sin(\alpha - \alpha_k) - x_w \cdot H \cdot \sin(\alpha - \alpha_k) + \\ & + y_w \cdot H \cdot \cos(\alpha - \alpha_k) \end{aligned} \tag{6}$$

Tilt moment from horizontal ballast

$$\begin{aligned} Mzsp = {} & x_{sp} \cdot Lsp \cdot \cos(\alpha_k - \Delta\varepsilon_{sp}) + \\ & + y_w \cdot Lsp \cdot \sin(\alpha_k - \Delta\varepsilon_{sp}) + \\ & + x_w \cdot Dsp \cdot \sin(\alpha_k - \Delta\varepsilon_{sp}) + \\ & + yw \cdot Dsp \cdot \cos(\alpha_k - \Delta\varepsilon_{sp}) \end{aligned} \tag{7}$$

Assuming that the moment from the horizontal stabilizer comes only from its lifting force (this assumption is reasonable because the effect of the drag force on the moment on the tilt moment is small due to at least the small value of the ysp arm of the drag force), the last formula can be written in the form:

$$Mzsp = x_{sp} \cdot Lsp \tag{8}$$

We will express the lifting force of the horizontal stabilizer with the help of the following formula:

$$Lsp = Ksp \cdot \frac{1}{2} \cdot \rho \cdot V^2 \cdot C_{L}sp, \tag{9}$$

$$\sqrt{Ksp} = \frac{Vsp}{V} \tag{10}$$

where: Ksp – a factor that takes into account the change in the velocity of the inflow of the undisturbed jet on the horizontal ballast.

Based on the tunnel test materials of the airframe model [15], the value of the product of KspCLsp is determined, which represents the coefficient of the horizontal stabilizer lift force related to the square of the airframe's airspeed. Usually, the value of the horizontal stabilizer lifting force is determined from the difference of the tilting moment of the airframe with and without the stabilizer. As a result, a family of curves of the dependence of KspCLsp on the angle of attack of the ballast for different angles of attack of the fuselage k is obtained. A typical dependence of the horizontal stabilizer lift coefficient on the angle of attack is shown in Figure 1.

The angle of attack of the horizontal stabilizer [16] will be expressed by the formula :

$$\alpha_{sp} = \alpha_k + \varepsilon_{sp} - \Delta\varepsilon_{sp} \tag{11}$$

where: ε_{sp} – Horizontal ballast setting angle (see Figure 1),
$\Delta\varepsilon_{sp}$ – Angle of slant of the inflow of undisturbed stream on the ballast.

The bevel is caused by the lifting rotor, fuselage and propeller.

The flux bias caused by the lifting rotor [15] can be expressed by the formula:

$$\Delta\varepsilon_{spw} = \kappa_{c0} \cdot \frac{2v_0}{V} \tag{12}$$

where: v_0 – average induced speed of the rotor,
V – the horizontal component of the windmill's airspeed,
κ_{c0} – coefficient that depends on the distance of the horizontal stabilizer yc0 to the center of the vortex plane descending from the lifting rotor and can be determined from the relationship shown in the diagram.

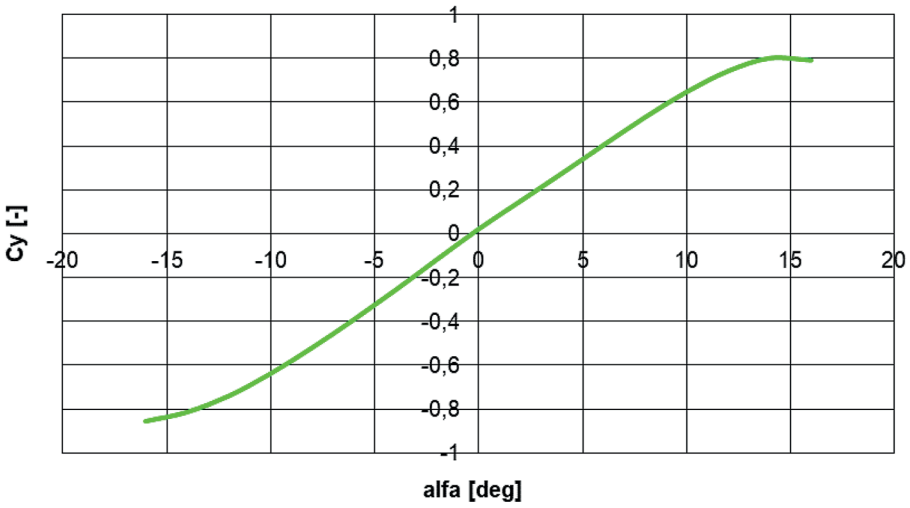

Fig. 1. Typical dependence of the lift coefficient of a horizontal ballast on its angle of attack

The magnitude of yc0 is determined according to the formula:

$$y_{c0} = (y_w - y_{sp}) + (x_w - x_{sp}) \cdot \sin(\alpha_k) \quad (13)$$

The above formula is obtained assuming that the induced velocity behind the rotor is twice that in the rotor plane.

The slope of the jet inflow to the horizontal ballast $\Delta\varepsilon_{spk}$ from the fuselage spk depends on the fuselage angle of attack α_k. The relationship $\Delta\varepsilon_{spk}=f(\alpha_k)$ is determined on the basis of the results of tunnel tests of the windmill model. At the points of intersection of the curves $m_{zk+sp}= f(\alpha_k)$ for the model without a horizontal stabilizer with the curves mzk+sp= f(k) for the fuselage with a horizontal stabilizer for different angles of attitude (Fig. 2). At the points of intersection, the condition $C_{Lsp} = 0$ occurs, and hence we get the following [17]:

$$\alpha_0 = \varepsilon_{sp} + \alpha_k - \Delta\varepsilon_{sp} \quad (14)$$

$$\Delta\varepsilon_{sp} = \varepsilon_{sp} + \alpha_k - \alpha_0 \quad (15)$$

where: α_0 – angle of zero lift force of the horizontal stabilizer (can be assumed equal to zero).

If we do not have the results of model measurements in the wind tunnel, then we can assume the relation $\Delta\varepsilon_{spk}= f(\alpha_k)$ for an eddyplane with similar shapes of the fuselage and horizontal ballast. An example of the dependence of the angle

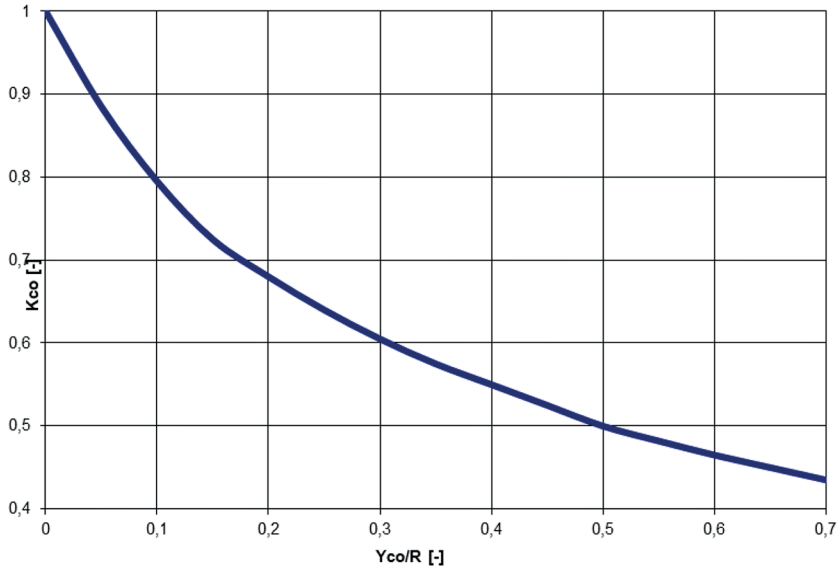

Fig. 2. Induction coefficient of the carrier rotor on the horizontal ballast

of slant of the incoming jet on the horizontal ballast caused by the fuselage is shown in Figure 3b.

We will assume the effect of the propeller on the contrail by geometrically summing the doubled induced velocity of the propeller and the inflow velocity of the undisturbed jet [18]. Then the inflow velocity on the ballast will be expressed by the formula:

$$Vsp = \sqrt{4v_s{}^2 + V^2 + 2 \cdot \cos(\alpha_k + \varepsilon_s)} \qquad (16)$$

And the bevel angle from the propeller to the horizontal stabilizer is calculated using the formula:

$$\Delta\varepsilon_{sps} = arc\sin[\frac{2vs}{Vsp} \cdot \sin(\alpha_k + \varepsilon_s)] \qquad (17)$$

where: *vs* – denotes the induced velocity of the propeller in the plane of rotation of the propeller

Formula (17) expresses the angle formed by the geometric sum of the doubled propeller induced velocity and velocity of the undisturbed stream with the inflow velocity of the undisturbed. If we use a conservative approach, the effect of the propeller on the horizontal ballast can be disregarded (ΔVsp = 0).

As mentioned above in the course of aerodynamic calculations, we calculate the forces on the lifting rotor T, H and calculate the propeller thrust ensuring the fulfillment of equations (1) and (2) with the simultaneous condition that the rotor operates on autorotation, which is equivalent, the condition Myp=0. The task is to determine such rotor angle of attack and rotor pitch angle (for a rotor with overall pitch control) or such rotor rotation (rotor without pitch control) at which the balance of forces in the longitudinal plane of the windmill will be satisfied.

With the balance of forces in the longitudinal plane determined, we can determine the

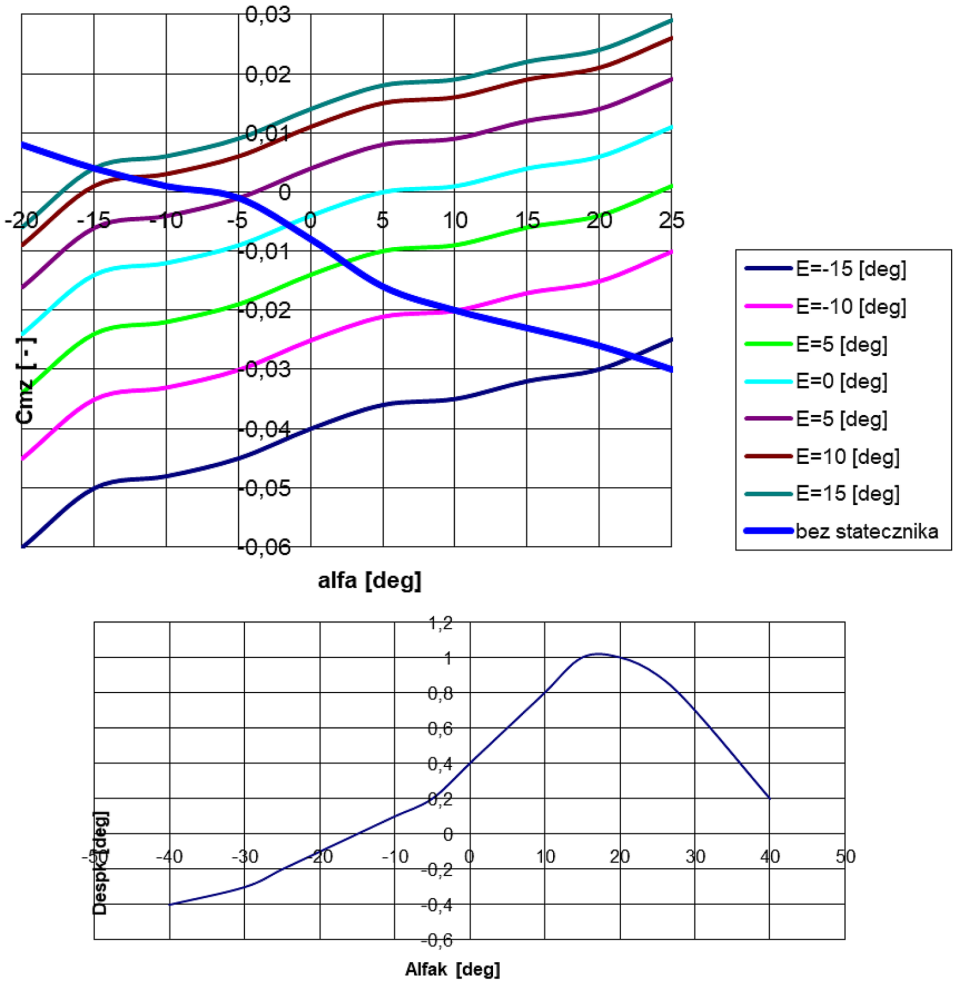

Fig. 3. (a) Hull leaning moment coefficient; (b) angle of slant of the jet inflow on the horizontal ballast from the fuselage

components Mzk, Mzs, Mzw of the equation of moments (3) according to equations (4), (5) and (6).

Then, from equation (18), we determine the moment Mzsp ensuring that the sum of moments will be zero (equation will be satisfied (3)).

$$Mzsp = -Mzs - Mzk - Mzw \tag{18}$$

Having calculated this value, we determine the lifting force coefficient of the horizontal stabilizer according to the relation:

$$C_{Lsp} = \frac{Mzsp}{x_{sp} \cdot \frac{1}{2}\rho(V + \Delta Vsp)^2 \cdot Ssp} \tag{19}$$

Then, from the polar (Fig. 4), we determine the angle of attack of the ballast corresponding to the determined lift coefficient and, based on the above-quoted formulas, we calculate the jet bevel angles from the rotor, fuselage and propeller of the windmill and finally calculate the necessary ballast angle for equilibrium according to the following formula:

$$\varepsilon_{sp} = \alpha_{sp} - \alpha_k + \Delta\varepsilon_{sp} \tag{20}$$

It should be noted that at low airspeeds the horizontal stabilizer lift coefficient required for equilibrium will be greater than CLmax (less than CLmin), then the equilibrium of the windmill moments is not possible.

SEQUENCE OF LONGITUDINAL STABILITY CALCULATIONS

Longitudinal static stability calculations can be performed in the following order:

1. Determine the angle of the flight trajectory – $\theta = \text{arctg}(Vy/Vx)$
2. Assume the value of the angle of inclination of the hull – υ
3. Calculate the angle of attack of the fuselage – $\alpha_k = \upsilon - q$
4. We make aerodynamic calculations of the rotor. As a result of them, we calculate, among other things, the forces T and H, Ts satisfying the balance of forces in the plane of symmetry of the windmill with the condition of rotor autorotation, and determine the angle of attack of the rotor. Having the angle of attack of the rotor, we can calculate the angle A1W by which the axis of the carrier rotor should be deflected from its initial position – $A1W = \alpha - \alpha_k - \varepsilon_w$ from Figure 1. we can determine the value of the rotor thrust force T and the propeller thrust force Ts that provide the balance of forces in the plane of symmetry of the windmill:

$$T = G \cdot \cos(\theta + \alpha) + Ts \cdot \sin(\alpha - \alpha_k - \varepsilon_s) - \\ - L_k \cdot \cos(\alpha) - D_k \cdot \sin(\alpha) - Lsp \cdot \cos(\alpha) \tag{21}$$

$$Ts = G \cdot \sin(\vartheta + \varepsilon_s) - L_k \cdot \sin(\alpha_k + \varepsilon_s) + \\ + D_k \cdot \cos(\alpha_k + \varepsilon_s) + T \cdot \sin(\alpha - \alpha_k - \varepsilon_s) + \\ + H \cdot \cos(\alpha - \alpha_k - \varepsilon_s) - Lsp \cdot \sin(\alpha_k + \varepsilon_s) \tag{22}$$

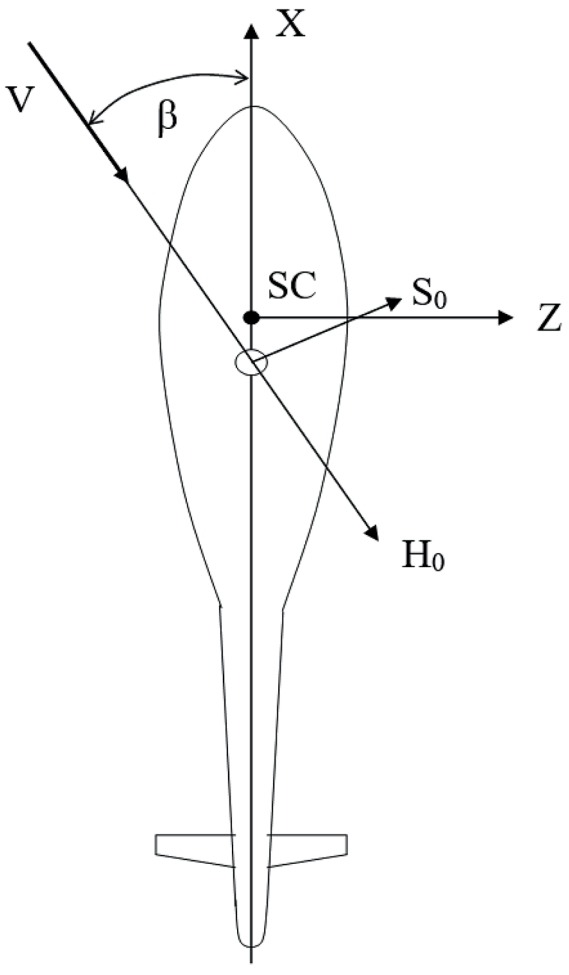

Fig. 4. Definitions of parameters in flight with glide angle

In the above formulas, there is no drag force from the horizontal stabilizer, since the fuselage drag is taken into calculations including the stabilizer. The two equations are mutually dependent – in (21) the thrust T is dependent on the propeller thrust Ts, while in (22) the thrust Ts is dependent on T. Since the iteration method is used in the rotor calculations, this problem does not occur or unpowered flight (propeller thrust Ts=0), the windmill performs a descending flight. We determine the angle of the flight trajectory from the following equation:

$$\theta = -\alpha + ar\,\mathrm{ctg}\left(\frac{-H - D_k \cdot \cos(\alpha) + L_k \cdot \sin(\alpha) + L_{sp} \cdot \sin(\alpha)}{T + D_k \cdot \sin(\alpha) + L_k \cdot \cos(\alpha) + L_{sp} \cdot \cos(\alpha)}\right)$$

This equation is obtained when the sum of the force projections perpendicular to the rotor axis is divided by the sum of the force projections on the rotor axis shown in the following equations.

$$m \cdot g \cdot \sin(\theta + \alpha) = -H - D_k \cdot \cos(\alpha) + L_k \cdot \sin(\alpha) + L_{sp} \cdot \sin(\alpha)$$
$$m \cdot g \cdot \cos(\theta + \alpha) = T + D_k \cdot \sin(\alpha) + L_k \cdot \cos(\alpha) + L_{sp} \cdot \cos(\alpha)$$

Having the angle of the trajectory, the vertical velocity will be determined from the relationship: $Vy = V \cdot \sin(\theta)$.

From the equation of moments, we calculate the required angle of the horizontal stabilizer for the preservation of the fixed set inclination of the fuselage υ.

As a result of the calculations, for each assumed fuselage pitch angle, the rotor axis yaw angle A1W and the horizontal stabilizer attitude angle will be determined ε_{sp}.

It should be noted that the above cycle of calculations is performed for the given:

- the horizontal component of the windmill's flight speed – Vx,
- vertical component of the windmill's flight speed – Vy,
- pressure altitude of the windmill's flight – H,
- ambient temperature under flight conditions – TH,
- mass and position of the windmill's center of gravity in flight M, XT, YT, ZT.

As a result of the calculation of longitudinal static stability for a given flight altitude, we will obtain, among other things, the relation A1W = f(V), the so-called equilibrium curve. If its gradient after the flight speed is negative, we say that the windmill is statically stable.

LATERAL STABILITY

The condition of lateral equilibrium of the windmill is the balance of moments with respect to the vertical and horizontal axes and the balance of the projections of forces on the lateral axis:

ΣMy=0, ΣMx=0, ΣZ=0.

The sum of ΣMy moments consists of the following components :

- rotor reaction torque (practically equals zero, since the rotor operates under autorotation conditions. It is only possible to take into account the moment from frictional resistance in the rotor rotation system),
- moment from the lateral force of the rotor,
- aerodynamic moment of the airframe,
- moment from the vertical stabilizer – rudder.

Therefore, the equation ΣMy=0 can be written:

$$Myw + Myk + Mykil = 0 \qquad (23)$$

As an analogy to this equation, we will represent ΣMx=0 and ΣZ=0 in the form of:

$$Mxs + Mxw + Mxk + Mxkil = 0 \qquad (24)$$

$$Zw + Zk + G \cdot \cos\upsilon \cdot \sin\gamma + \Delta Pzkil = 0 \qquad (25)$$

We can write equation (25) in approximate terms:

$$Zw + Zk + G \cdot \gamma + \Delta Pzkil = 0 \qquad (26)$$

The following will give the relationships for the forces and moments found in the equations (23), (26).

$$Zw = H_0 \cdot \sin(\beta) + S_0 \cdot \cos(\beta) + T \cdot B1W \qquad (27)$$

The lateral force of the lifting rotor in glide flight can be represented as the sum of the projections on the associated windmill axis OZ of the lateral and longitudinal rotor forces S_0 and H_0 with the rotor axis not tilted back (Fig. 6).

where: $H_0 = H - T \cdot \Delta A1W$,

$S_0 = S$, $B1W$ – rotor shaft axis tilt angle,

ΔA1W – increase in the rotor axis yaw angle due to the increase in the aerodynamic moment of the airframe in flight with the glide angle β.

The aerodynamic characteristics of the fuselage entering the calculation are determined in the coordinate axis system associated with the windmill. When determining the characteristics in the tunnel, the fuselage is complete, i.e., with the vertical contrail (vertical stabilizer). Therefore, in Equation 23, *Myki*l means the increment of moment from the increment of lateral force Δ*Pzkil* due to directional injection necessary to satisfy Equation 23.

$$Zk = \frac{1}{2} \cdot \rho V^2 F \cdot Czk \tag{28}$$

$$Myk = \frac{1}{2} \cdot \rho V^2 F \cdot R \cdot Cmyk \tag{29}$$

$$Mxk = \frac{1}{2} \cdot \rho V^2 F \cdot R \cdot Cmxk \tag{30}$$

RESULT OF CALCULATION

Example dependencies of lateral force coefficients Czk, yawing moment Cmyk, fuselage tilting moment Cmxk are shown in the following diagrams Figures 5, 6 and 7.

With lateral streamlining of the airframe, there is an increase in the aerodynamic tilting moment, which must be balanced by additional backward deflection or tilt of the rotor shaft axis.

This graph shows the relationship $\Delta mzk=mzk(\alpha_k, \beta) - mzk((\alpha_k, \beta=0)$.

Figure 8 shows an example of the dependence of the increase in the aerodynamic tilt moment coefficient Dczmk as a function of the glide angle β and fuselage angle of attack α_k

The moments are expressed by the following relationships:

$$Myw = -Myop \cdot P - Zw \cdot xw \tag{31}$$

$$Mykil = -\Delta Pzkil \cdot xkil \tag{32}$$

$$Mxs = -Ps / \omega s \cdot P1 \tag{33}$$

$$Mxw = Zw \cdot Yw - T \cdot zw \tag{34}$$

$$Mxkil = \Delta Pzkil \cdot ykil \tag{35}$$

In the above formulas, P and P1 are control parameters. If the rotor rotation is counterclockwise when viewed from above then P=1, otherwise P= -1. When the propeller rotation is clockwise when viewed in the direction of flight when viewed from the rear of the windmill then P1=1, otherwise P1= – 1. Using the formulas written above, we can perform lateral equilibrium calculations. The usual calculation range of glide angle β = 20 to 25 degrees with a step of 5 degrees is adopted.

In order to obtain the increment of lateral force ΔP_{zkil} on the vertical ballast, the vertical ballast must be properly set to angle ε_k. The angle ε_k can be determined from the following formula:

$$\varepsilon_k = \frac{\Delta P_{zkil}}{\frac{1}{2} \rho V_k{}^2 S_k \cdot a_k} \tag{36}$$

where: V_k the inflow velocity of the airstream on the vertical ballast, which can be taken as the sum of the airspeed and the velocity of the propeller jet *Vsp*, expressed by the formula (16)

$$a_k = \frac{\partial Cz_{kil}}{\partial \varepsilon}$$

The gradient of the lifting force of the vertical stabilizer after its control angle. When the vertical stabilizer is controlled by its rotation with respect to its twist axis, ak is the gradient of the lifting force after the angle of attack and otherwise after the angle of deflection of the control surface.

In the case of a butterfly lip, the lateral force is obtained by differentially deflecting the control surfaces by an angle ε_k. Then the lateral force is obtained (according to Figure 9):

$$\Delta P_{zkil} = 2 \cdot \Delta L_k \cdot \sin(\psi_k) \tag{37}$$

$$\Delta L_k = \frac{1}{2} \rho \cdot V_k{}^2 \cdot \frac{S_k}{2} \cdot a_k \cdot \varepsilon_k \tag{38}$$

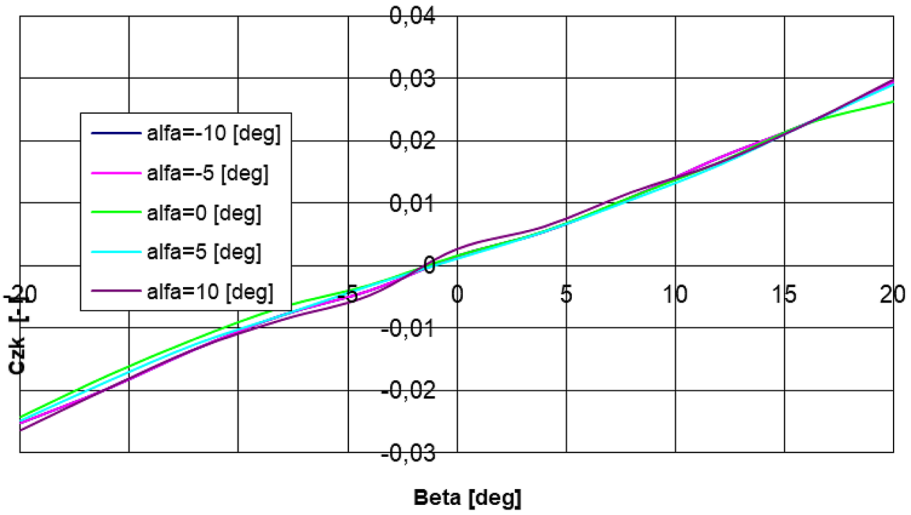

Fig. 5. Lateral force coefficient of the airframe

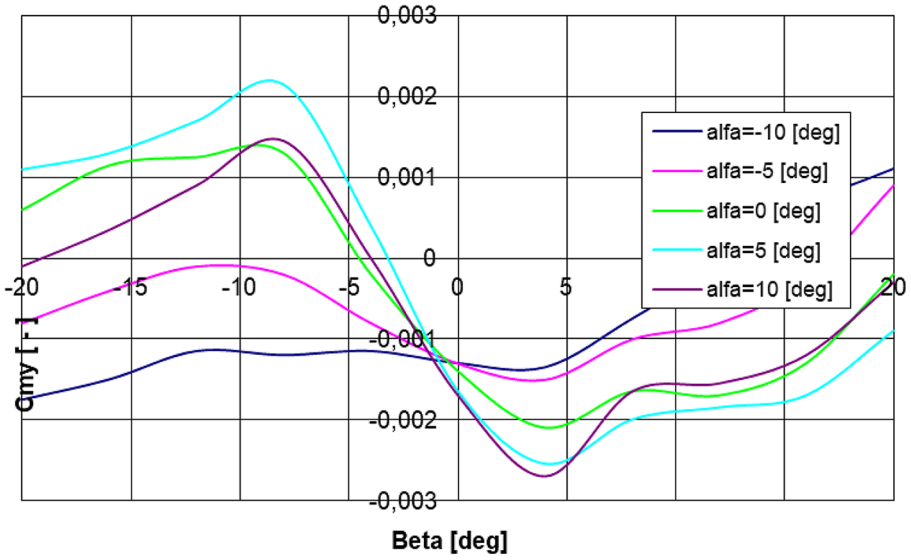

Fig. 6. Airframe deflection moment coefficient

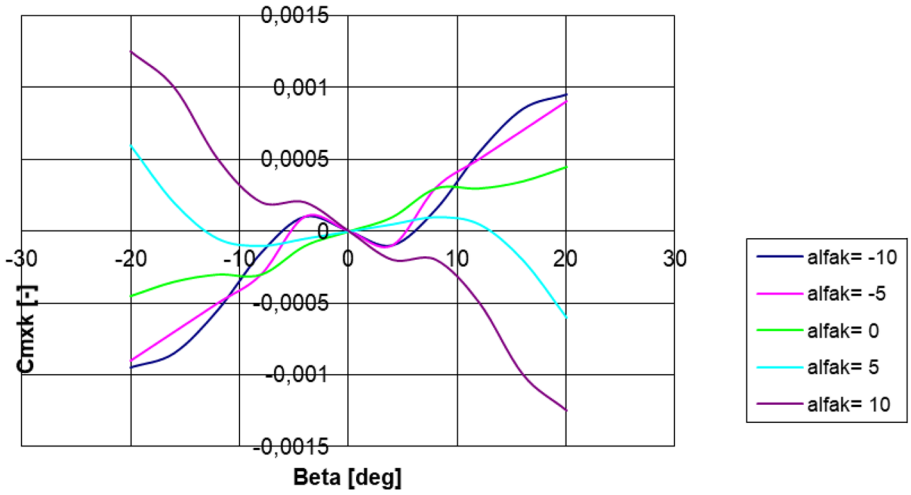

Fig. 7. Tilting moment coefficient

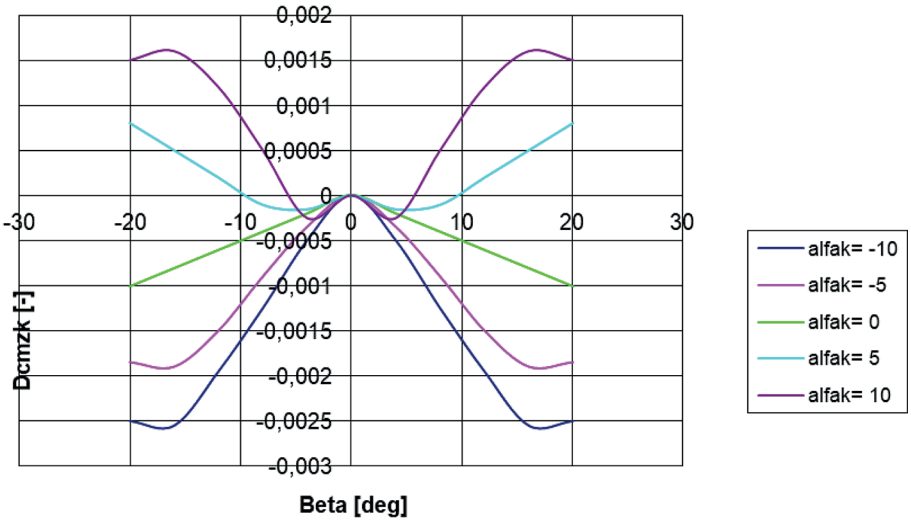

Fig. 8. Hull pitching moment increment factor

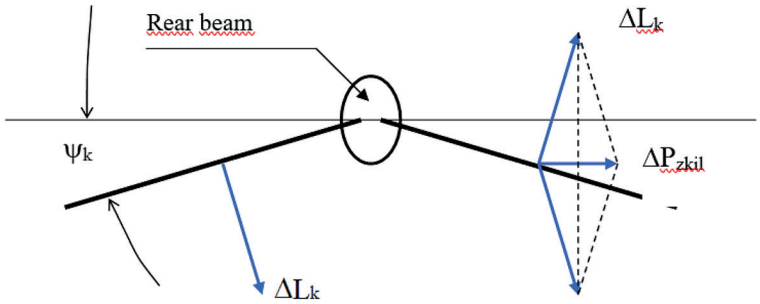

Fig. 9. Determination of lateral force increment from directional injection

From equations (37) and (38), we can determine the required differential injection angle according to the following formula:

$$\varepsilon_k = \frac{\Delta P_{zkil}}{2 \cdot \frac{1}{2} \rho \cdot V^2{}_k \cdot \frac{S_k}{2} \cdot a_k \cdot \sin(\psi_k)} = \frac{\Delta P_{zkil}}{\frac{1}{2} \rho \cdot V^2{}_k \cdot S_k \cdot a_k \cdot \sin(\psi_k)} \tag{39}$$

EXAMPLE OF THE RESULTS OF HORIZONTAL FLIGHT STABILITY CALCULATIONS

Longitudinal stability related to the balance of forces and moments in the plane of symmetry includes:

- A1W dependence on airspeed
- Dependence of horizontal stabilizer attitude angle on airspeed.

As can be seen from Figure 10, the wind turbine is characterized by static stability – an increase in airspeed must be accompanied by a forward tilt of the carrier rotor axis.

Figure 10 also shows the effect of the fuselage tilt angle on the value of the rotor axis yaw angle – an increase in the υ_K angle (an increase in the rump angle) causes a decrease in the backward yaw of the rotor axis. This is even intuitively understandable – the rotor angle of attack for a fixed airspeed practically does not depend on the υ_K angle, unless the aerodynamic characteristics of the airframe strongly depend on its angle of attack.

It should be noted that for the fuselage angle υ and at flight speeds greater than 190 km/h, a forward tilt of the rotor axis (A1W<0) is required for the balance of the windmill. Normally, the design of a windmill aircraft does not allow the rotor axis to tilt forward. Therefore, a forward tilt of the windmill ($\upsilon < 0$) will be required to maintain flight speeds greater than 190 km/h.

As can be seen from Figure 11, large horizontal stabilizer attitude angles are required to balance the tilting moment of the windmill at

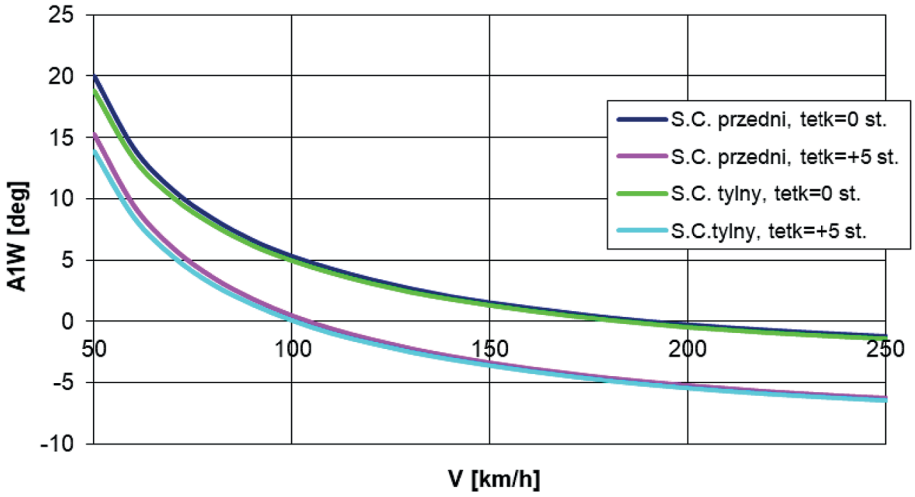

Fig. 10. Dependence of the angle of deflection of the axis of the lifting rotor shaft on the flight speed of the windmill

low airspeeds, which may exceed the maximum design values. As can be seen from Figure 11, increasing the fuselage angle υ_k reduces the required horizontal ballast ε_{sp} attitude angle. Hence, it follows that at low speeds of horizontal flight, such a situation may occur when the angle of the horizontal stabilizer reaches the maximum design value, then to ensure the balance of the windmill the hull angle will be increased.

This effect is caused by the difference in the rotor angle of attack – the rotor angle of attack is greater in the flight of a windmill with a forward center of gravity position.

Lateral stability

Below are graphs showing selected lateral equilibrium curves, i.e. the dependence on the glide angle and for flight speeds V= 50, 100, 150, 200 and 250 km/h of the required tilt of the axis of the lifting rotor shaft sideways B1W (Fig. 12) and the tilt angle of the windmill in flight with the glide (Fig. 13) for the above flight speeds.

CONCLUSIONS

The results of the obtained tests allowed to determine the static stability of this type of object and can be used for comparison against other newly aircraft gyrocopter. The dependence of the lifting rotor speed on the horizontal flight speed of the windmill for a rotor was found – the rotor speed increases with the flight speed. At the same time, we showed that in flight with the rear center of gravity

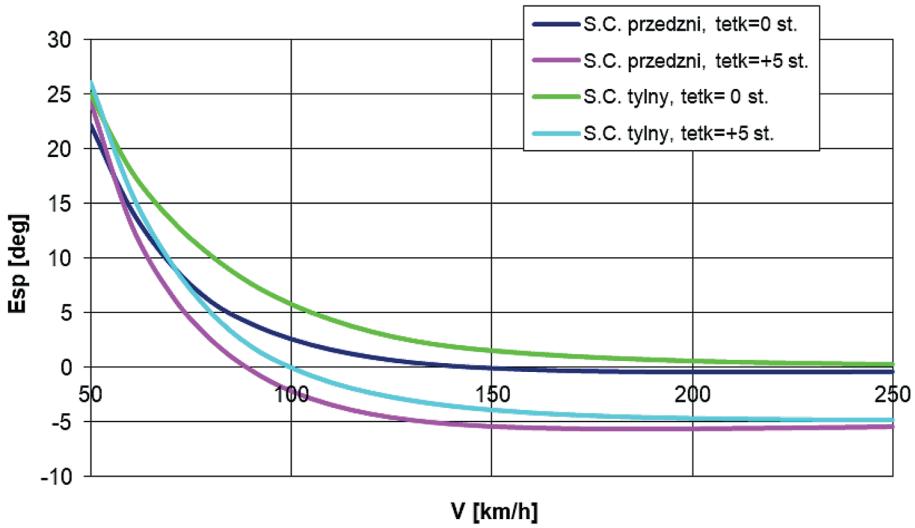

Fig. 11. Dependence of horizontal stabilizer attitude angle on windmill flight speed

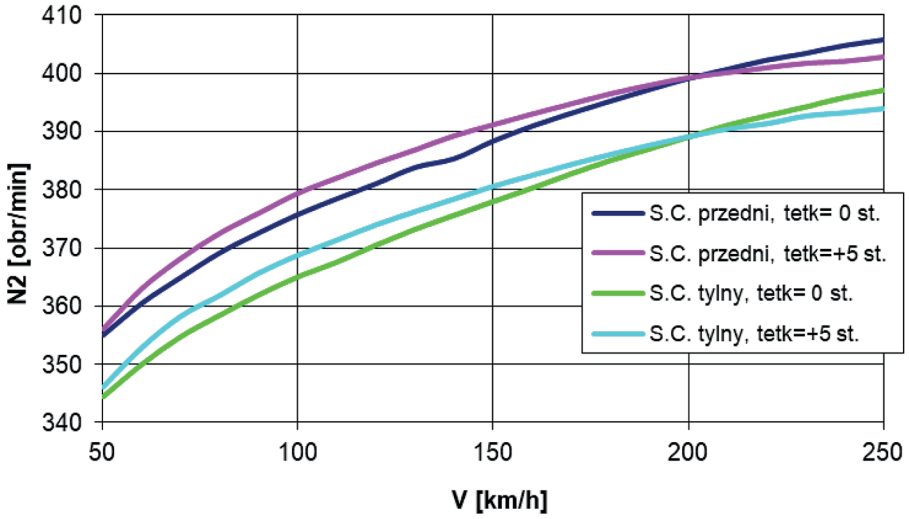

Fig. 12. Dependence of carrier rotor speed on gyroplane airspeed

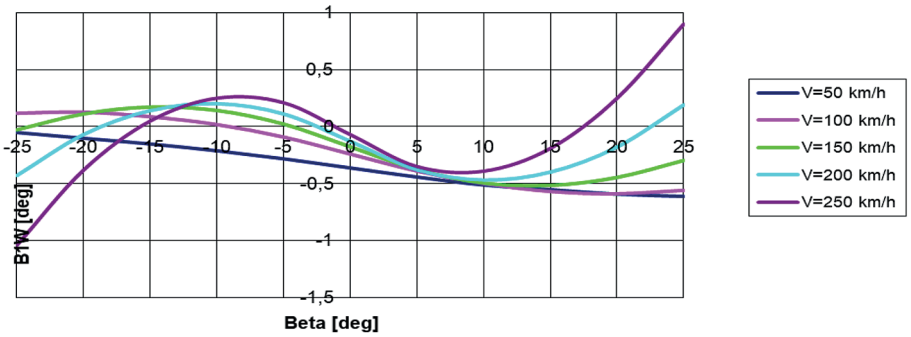

Fig. 13. Precession to the side of the WN shaft axis (>0 to the right), S.C. front

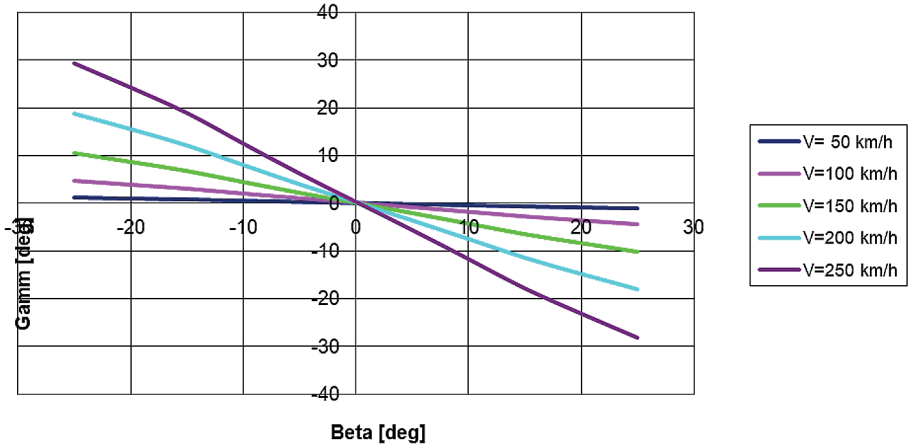

Fig. 14. Hull roll angle (>0 right), S.C. forward, tetk=0 deg

position, the rotor rpm is lower than in flight with the front balance of the windmill.

The parameters waveforms were determined in the range of the glide angle –25 ° ≤ β ≤ +25°. If at low speeds this range of glide angle can be practical (useful), then at high flight speeds large glide angles must be accompanied by significant fuselage tilt. For example, at an airspeed of V = 250 km/h and with glide β =+10 degrees (left inflow), the windmill would have to be tilted to the left – roll angle γ = -12°. Therefore, at high airspeeds, the pilot will avoid flying with glide.

From the point of view of control reserves, consider the relationship of the required B1W angle of tilt to the side of the carrier rotor axis was shown. The angle magnitudes shown in this

research must be less than the design limitations. The control reserve is usually assumed to be 10–20% of the full control range in each string. For example, if the design range of the rotor shaft axis tilt is B1Wmax = ± 5 degrees, the B1W control reserve should be at least 1–2 degrees, so the side control reserve is much larger than required.

REFERENCES

1. Abłamowicz A., Nowakowski W. Fundamentals of aerodynamics and flight mechanics, 2014.
2. Anderson Jr. J.D. Fundamentals of Aerodynamics, McGraw-Hill International, 2016
3. Araujo-Estrada S.A., Lowenberg M.H., Neild S.A. Capturing nonlinear time-dependent aircraft dynamics using a wind tunnel manoeuvre rig, Bristol, 2022.
4. Bertin J.J., Cummings R.M. Aerodynamics for Engineers, Wydawnictwo Pearson, 2019.
5. Goraj Z., Figat M. Analysis of the concept in terms of aerodynamic and corkscrew properties of the AT-5 aircraft. Stage I and II, Warsaw University of Technology, 2018
6. Kowaleczko G. Reconstruction of the last phase of TU-154M's flight, 2018
7. Kuethe A.M., Chow C-Y, Foundations of Aerodynamics: Bases of Aerodynamic Design, John Wiley & Sons Ltd, 2018
8. McLean D. Understanding Aerodynamics, John Wiley & Sons Ltd, 2016
9. Measuring and testing apparatus for experimental aerodynamics, Instruction manual, CTO S.A., 2021
10. Melnarowicz W. Aerodynamics and mechanics of flight. Part I Aerodynamics of Aircraft, 2018.
11. Ochal P. Rules of Flight, Aeroclub Bielsko-Bialski, 2020.
12. Olejnik A., Kachel S., Makowski W., Krzyżanowski A., Frant M., Skrodzki C. Experimental aerodynamic characteristics of the F-16 aircraft model in asymmetric flight, WAT Warsaw, 2018
13. Olejnik A., Krzyżanowski A., Kachel S., Frant M., Makowski W., Skrodzki C. Experimental aerodynamic characteristics of the F-16 aircraft model in symmetric flight, WAT Bulletin Warsaw, 2017.
14. Ramanan G., Radha Krishnan P., Ranjan H.M. An aerodynamic performance study and analysis of SD7037 fixed wing UAV airfoil, Bangalore, 2021
15. Rizzi A., Luckring J.M. Historical development and use of CFD for separated flow simulations relevant to military aircraft, Elsevier, 2021.
16. Zhenhao Z., Tianhang X., Haolin Z., Shuanghou D., Yujin L. Aerodynamic characteristics of co-flow jet wing with simple high-lift devices, Chiny, 2021.